Surface Charge and Calcium Channel Saturation in Bullfrog Sympathetic Neurons

WEI ZHOU and STEPHEN W. JONES

From the Department of Physiology and Biophysics, Case Western Reserve University, Cleveland, Ohio 44106

ABSTRACT Currents carried by Ba^{2+} through calcium channels were recorded in the whole-cell configuration in isolated frog sympathetic neurons. The effect of surface charge on the apparent saturation of the channel with Ba^{2+} was examined by varying $[Ba^{2+}]_o$ and ionic strength. The current increased with $[Ba^{2+}]_o$, and the *I-V* relation and the activation curve shifted to more positive voltages. The shift of activation could be described by Gouy-Chapman theory, with a surface charge density of 1 e^-/140 $Å^2$, calculated from the Grahame equation. Changes in ionic strength (replacing *N*-methyl-D-glucamine with sucrose) shifted the activation curve as expected for a surface charge density of 1 e^-/85 $Å^2$, in reasonable agreement with the value from changing $[Ba^{2+}]_o$. The instantaneous *I-V* for fully activated channels also changed with ionic strength, which could be described either by a low surface charge density (less than 1 e^-/1,500 $Å^2$), or by block by NMG with $K_d \sim 300$ mM (assuming no surface charge). We conclude that the channel permeation mechanism sees much less surface charge than the gating mechanism. The peak inward current saturated with an apparent K_d = 11.6 mM for Ba^{2+}, while the instantaneous *I-V* saturated with an apparent K_d = 23.5 mM at 0 mV. This discrepancy can be explained by a lower surface charge near the pore, compared to the voltage sensor. After correction for a surface charge near the pore of 1 e^-/1,500 $Å^2$, the instantaneous *I-V* saturated as a function of local $[Ba^{2+}]_o$, with K_d = 65 mM. These results suggest that the channel pore does bind Ba^{2+} in a saturable manner, but the current-$[Ba^{2+}]_o$ relationship may be significantly affected by surface charge.

INTRODUCTION

Two fundamental questions about ion channels are the mechanisms underlying gating (when is a channel open?) and permeation (how do ions go through an open channel?). It has long been recognized that these processes can be affected by the presence of charged groups in the vicinity of the channel (Frankenhaeuser and Hodgkin, 1957; Hille, 1968; for reviews, see McLaughlin, 1977; Green and Anderson, 1991; Hille, 1992). Such surface charges were classically thought to be negative charges on the head groups of phospholipids, and were described using Gouy-

Address correspondence to S. W. Jones at Department of Physiology and Biophysics, Case Western Reserve University, Cleveland, OH 44106.

J. GEN. PHYSIOL. © The Rockefeller University Press · 0022-1295/95/04/0441/22 $2.00
Volume 105 April 1995 441–462

Chapman theory assuming a uniform planar distribution of charge (Grahame, 1947; Gilbert and Ehrenstein, 1969), but it is now recognized that charged groups on the channel protein may also act as surface charges. Effects of surface charge on gating have been studied extensively, but effects on permeation have been less thoroughly characterized, especially for calcium channels.

It is generally found that the current through a channel saturates as a function of the concentration of the ion carrying charge through the channel. It would seem natural to interpret this as saturation of a binding site within the channel pore, presumably a site involved in determining the ion selectivity of the channel, so saturation might provide important clues about channel structure. However, surface charge can influence the current-concentration curve. The observed saturation of calcium channels with Ba^{2+} can be explained partially or entirely by the effect of surface charge (Ohmori and Yoshii, 1977; Wilson, Morimoto, Tsuda, and Brown, 1983; Cota and Stefani, 1984; Byerly, Chase, and Stimers, 1985; Ganitkevich, Shuba, and Smirnov, 1988; Smith, Ashcroft, and Fewtrell, 1993). For sodium channels, it is possible to describe the shape of the current-$[Na^+]_o$ curve either in terms of surface charge, or as saturation of binding site(s) in the pore (Green, Weiss, and Anderson, 1987; Cai and Jordan, 1990; Ravindran, Kwiecinski, Alvarez, Eisenman, and Moczydlowski, 1992; Naranjo and Latorre, 1993).

In the present study, we have examined the effects of changes in $[Ba^{2+}]_o$ and ionic strength on calcium channel currents in frog sympathetic neurons, using the whole-cell patch clamp technique. We estimated the effects of surface charge on gating and permeation, using the activation curve measured from tail currents to study gating, and the instantaneous *I-V* curve after strong depolarizations to study permeation. Analysis using Gouy-Chapman theory indicates that the permeation mechanism sees less surface charge than the gating mechanism. The results also suggest that the current carried by Ba^{2+} saturates, but at higher concentrations than estimated from measurements from the peak *I-V* relations. That is, the apparent saturation of current through the calcium channel depends partially (but not entirely) on effects of surface charge.

METHODS

Neurons were isolated from paravertebral sympathetic ganglia of adult bullfrogs (*Rana catesbeiana*), and maintained in culture at 4°C, as described previously (Kuffler and Sejnowski, 1983; Jones and Marks, 1989). Currents were recorded in the whole-cell configuration (Hamill, Marty, Neher, Sakmann, and Sigworth, 1981). The standard intracellular solution contained (in millimolar) 82.6 *N*-methyl-D-glucamine chloride (NMG·Cl), 2.5 NMG·HEPES, 10 NMG_2·EGTA, 5 $Tris_2$·ATP, and 6 $MgCl_2$, titrated to pH 7.2 with NMG base. Extracellular solutions are given in Table I. The holding potential was −80 mV unless otherwise noted. Leakage and capacitative currents were subtracted using inverted and scaled currents from hyperpolarizing voltage steps (usually one fourth of the amplitude of the depolarizations used). Currents were filtered at 3 kHz unless otherwise noted. All experiments were carried out at room temperature. Data were acquired using pClamp software and Labmaster A-D boards from Axon Instruments, Inc. (Foster City, CA). Data analysis was with pClamp and locally written programs on IBM X86-compatible microcomputers.

In experiments varying ionic strength, a 3 M KCl agar bridge was used as the reference electrode. When Ba^{2+} concentrations were changed, a solid Ag/AgCl pellet was used. Small

changes in junction potential (<4 mV) were found to develop at the pellet in solutions with different $[Ba^{2+}]_o$. Data are shown without correction for these junction potentials, except for the calculated voltage shift-$[Ba^{2+}]_o$ and current-$[Ba^{2+}]_o$ relations.

We use ionic concentrations rather than activities, mainly because of uncertainty about activity coefficients in solutions of NMG·Cl. We estimate that this would tend to underestimate surface charge densities. However, using concentrations makes it easier to compare our results to previous studies, most of which also used concentrations rather than activities.

In these experiments, we wanted to analyze separately the effects of surface charge on gating and permeation. Effects on gating were assessed from activation curves (see Fig. 3 *A*), measured from tail currents at a fixed voltage (usually −40 mV) at 0.3–1.0 ms after termination of depolarizations to voltages from −70 to +80 mV (see Fig. 2 *B*). The tail current amplitudes were normalized to the tail current measured after the depolarization to +80 mV. The normalized currents should be equal to (or at least proportional to) the probability that the channel is open. Shifts in gating were measured from the changes in the midpoint of the activation curve.

TABLE I

Extracellular Solutions

	2 Ba	5 Ba	10 Ba	20 Ba	30 Ba	50 Ba
$BaCl_2$	2.0	5.0	10.0	20.0	30.0	50.0
NMG·Cl	117.5	113.0	105.5	90.5	75.5	45.5
NMG·HEPES	2.5	2.5	2.5	2.5	2.5	2.5

	10 NMG	40 NMG	117.5 NMG	250 NMG
$BaCl_2$	2.0	2.0	2.0	2.0
NMG·Cl	10.0	40.0	117.5	250.0
NMG·HEPES	2.5	2.5	2.5	2.5
Sucrose	215	155	0*	0

All concentrations are in millimolar. *In experiments with 250 mM NMG, the control extracellular solution (117.5 NMG) and the intracellular solution also contained 265 mM sucrose.

Effects on permeation were assessed using instantaneous *I-V* relations, measured from tail currents after 10-ms depolarizing pulses to +80 mV (Fig. 4, *A* and *B*). The initial tail current amplitude was measured either by fitting the tail current to a single exponential and extrapolating back to the end of the pulse to +80 mV, or by measuring the peak of the tail current. The two methods usually differed by <10% in the voltage range near 0 mV, which we used to determine the dependence of the instantaneous current on $[Ba^{2+}]_o$ or ionic strength.

The currents recorded were large, especially in high $[Ba^{2+}]_o$, which required careful attention to series resistance (R_s) error. Electrode tips were large (generally 3–5 μm) to maintain low R_s (0.8–3.5 MΩ before compensation). Routinely, 80–90% of R_s was compensated, using an Axopatch 200 patch clamp amplifier (Axon Instruments, Inc.). For one critical experiment, measurement of instantaneous *I-V* relations in high $[Ba^{2+}]_o$ (Fig. 4), the uncompensated R_s was 0.24, 0.2, and 0.5 MΩ in the three cells selected for analysis, producing estimated steady state errors of 4.6, 4.0, and 9.7 mV at 0 mV. Cells with signs of qualitative clamp error (unusually steep activation curves, or nonexponential tail currents beginning with a delay) were rejected from the analysis.

We and others have concluded previously that calcium currents are well isolated under our experimental conditions, and nearly all (~90%) of the whole-cell calcium current in frog

sympathetic neurons results from activity of N-type calcium channels, defined by sensitivity to ω-conotoxin GVIA (Jones and Marks, 1989; Werz, Elmslie, and Jones, 1993; see review by Jones and Elmslie, 1992). However, recent evidence indicates that a current resistant to ω-conotoxin GVIA appears in the presence of high $[Ba^{2+}]_o$ (Boland, Morrill, and Bean, 1994; Elmslie, Kammermeier, and Jones, 1994). That novel current is prominent at relatively negative voltages. Alignment of the *I-V* and activation curves (Figs. 2 *C* and 3 *A*) suggests that the novel current is detectable at ≥ 20 mM Ba^{2+}. In 50 mM Ba^{2+}, most of the current from -50 to -20 mV, and $\sim 10\%$ of the total conductance measured from tail currents, may be attributed to the novel current. Because our analysis concentrates on currents measured at 0 mV or more positive voltages, and on shifts in the midpoint of the activation curve, the novel current should have negligible effects on the results reported here. That is, our conclusions should be considered to apply to the N-type calcium current.

Most previous studies on surface charge and permeation in calcium channels have dealt with dihydropyridine-sensitive (L-type) calcium currents, or with calcium currents of invertebrates that may not fit into the classification schemes used for calcium channels of vertebrates. In fact, one motivation for undertaking this study was that these issues had not previously been studied in detail for N current. However, where direct comparision is possible, our results are not systematically different from previous reports on different calcium channel types, so possible differences among channel types will not be considered further.

Theory

Gouy-Chapman theory (reviewed by Hille, 1992) describes the relationship between the surface potential (Φ) and a uniform planar surface charge (σ) in an electrolyte solution. (The Discussion considers the limitations of Gouy-Chapman theory, as applied to ion channels.) If the only effect of ions is to screen the surface charges, the result is the Grahame equation (Grahame, 1947):

$$\sigma^2 G^2 = \Sigma[C_i]\{\exp(-z_i F\Phi/RT) - 1\} \quad (1)$$

where z_i is the valence of the i^{th} ion species, F is the Faraday constant, R is the gas law constant, and G is a constant equal to 270 $Å^2 e^{-1} M^{1/2}$ at room temperature. If ions are assumed to also bind to the surface charge, with association constants K_i (units/M^{-1}), the surface charge remaining after binding (σ) is related to the total surface charge (σ_t) by:

$$\sigma = \sigma_t/\{1 + \Sigma K_i[C_i] \exp(-z_i F\Phi/RT)\} \quad (2)$$

(Gilbert and Ehrenstein, 1969; Hille, Woodhull, and Shapiro, 1975; Wilson et al., 1983). Eqs. 1 and 2 were used to calculate the surface potential (Φ) for a given surface charge density (σ) and solution composition, using a numerical bisection method.

In this study, we consider two basic experiments, changes in $[Ba^{2+}]_o$, and changes in ionic strength with constant bulk $[Ba^{2+}]_o$. Fig. 1, *A* and *B*, show the predicted changes in surface potential ($\Delta\Phi$) as a function of the reciprocal of the surface charge density ($1/\sigma$). For changes in $[Ba^{2+}]_o$, $\Delta\Phi$ decreases monotonically with $1/\sigma$. However, when the concentration of NMG · Cl is changed (in the presence of 2 mM Ba^{2+}), $\Delta\Phi$ is a biphasic function of $1/\sigma$ (see Becchetti, Arcangeli, Del Bene, Olivotto, and Wanke, 1992). Qualitatively, with low σ the surface potential is small at all ionic strengths, with very high σ changes in ionic strength do not screen surface charge effectively, and the effect of ionic strength is maximal at intermediate σ.

Fig. 1 *C* illustrates the polarity convention. We define $\Delta\Phi$ as $\Phi_t - \Phi_c$, where Φ_t and Φ_c are the surface potentials in the test (t) solution and control (c) solutions, respectively (Fig. 1 *C*). A negative extracellular surface charge would produce a negative Φ, which would make the voltage seen by the channel more positive.

In principle, surface potentials could affect both gating and permeation. For gating, we

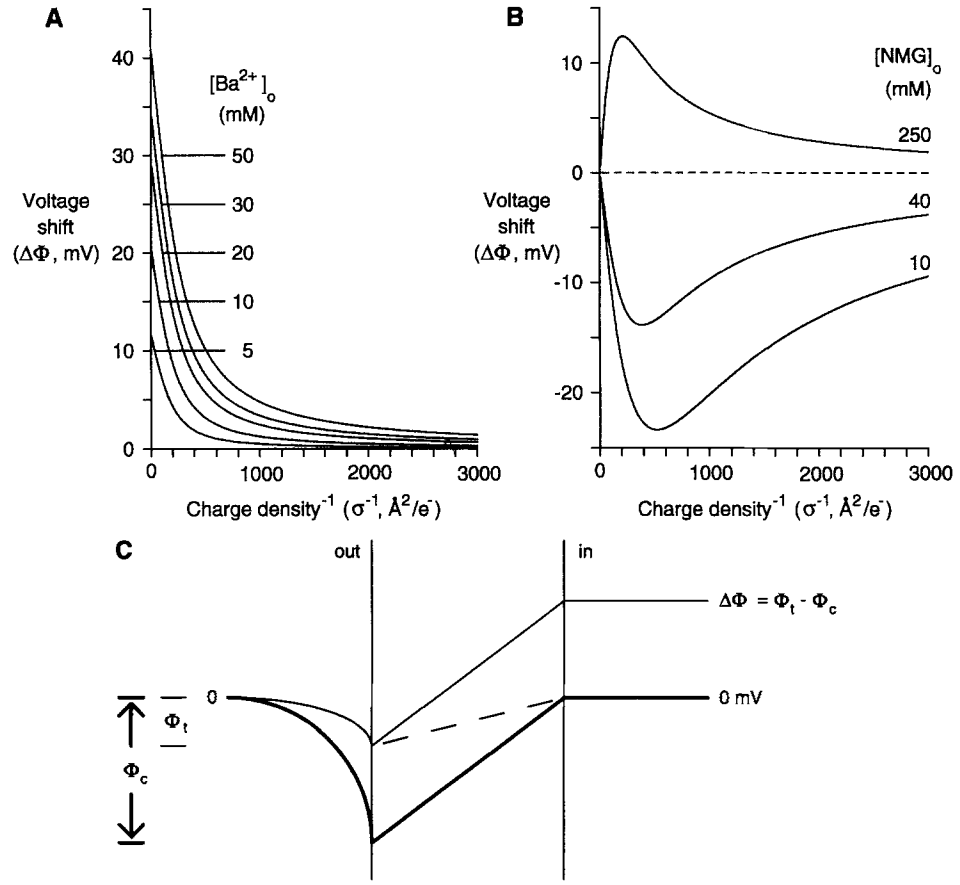

FIGURE 1. Changes in surface potential ($\Delta\Phi$) with surface charge (σ). (*A*) Effect of $[Ba^{2+}]_o$. (*B*) Effect of changes in ionic strength, with constant bulk $[Ba^{2+}]_o$. Values were calculated from the Grahame equation (Eq. 1), assuming no binding of Ba^{2+} to the surface charge (i.e., $K_{Ba} = 0$ in Eq. 2). $\Delta\Phi = \Phi_t - \Phi_c$, the surface potential in the experimental solution minus the surface potential in the control solution (2 mM Ba^{2+} and 117.5 mM NMG·Cl). Calculations included all ions present in the extracellular solution (Table I). (*C*) Effect of a negative extracellular surface charge. Two conditions are compared in control and test extracellular solutions, where the test solution screens more surface charge. The surface charge produces a negative surface potential, Φ_c or Φ_t. At a membrane potential of 0 mV, the voltage seen by the channel would be positive, $-\Phi_c$ in control, and $-\Phi_t$ in the test solution (*dashed lines*). The channel would see the same voltage in the control solution at 0 mV (*solid lines*) as at a membrane potential of $\Delta\Phi$ mV in the test solution (*narrow lines*). For clarity, no intracellular surface potential is shown.

assume that a surface potential simply shifts the probability that a channel is open along the voltage axis by Φ mV. Effects on permeation are more complex, as two effects are predicted (MacKinnon, Latorre, and Miller, 1989). First, the voltage profile seen by an ion as it moves through the channel is shifted by Φ mV. That is, we assume that the voltage across the channel is the macroscopic membrane potential minus the surface potential, Φ. For Ba^{2+} influx through a calcium channel, a negative surface potential would make the effective voltage across the channel more positive, decreasing the driving force on Ba^{2+} (see Fig. 1 *C*). Second, a negative

surface potential would increase the local concentration of a cation, according to the Boltzmann relation:

$$[C]_L = [C]_B \exp(-zF\Phi/RT), \tag{3}$$

where $[C]_L$ and $[C]_B$ are (respectively) the local and bulk ion concentrations.

For the experiments on ionic strength, we wished to calculate the change in current resulting from effects of surface charge on permeation. We allow for the possibility that the current through the channel saturates as a function of the local $[Ba^{2+}]_o$, as expected for a binding site with dissociation constant K_d. The ratio of the current in the test solution (I_t) to the control current (I_c) would be:

$$\frac{I_t}{I_c} = \frac{\left(\dfrac{I_{max}}{1 + K_d/Ba_{L,t}}\right)}{\left(\dfrac{I_{max}}{1 + K_d/Ba_{L,c}}\right)} = \frac{Ba_{L,t}(Ba_{L,c} + K_d)}{Ba_{L,c}(Ba_{L,t} + K_d)}$$

$$= \frac{Ba_t}{Ba_c} \exp(-2F\Delta\Phi/RT) \frac{Ba_c \exp(-2F\Phi_c/RT) + K_d}{Ba_t \exp\{-2F(\Delta\Phi + \Phi_c)/RT\} + K_d} \tag{4}$$

where the bulk $[Ba^{2+}]_o$ in control or test solution is Ba_c or Ba_t, and the local $[Ba^{2+}]_o$ is $Ba_{L,c}$ or $Ba_{L,t}$. With bulk $[Ba^{2+}]_o$ = 2 mM in both control and test solutions, and RT/F = 25.3 mV:

$$I_t = I_c \exp(-2\Delta\Phi/25.3) \frac{2 \exp(-2\Phi_c/25.3) + K_d}{2 \exp\{-2(\Delta\Phi + \Phi_c)/25.3\} + K_d} \tag{5}$$

For a given surface charge density, Φ_c and Φ_t (and thus $\Delta\Phi$) can be calculated from Eqs. 1 and 2. If the K_d is known, Eq. 5 can now be used to calculate the expected I_t corresponding to an experimental value of I_c. Because the change in surface potential also shifts the voltage profile within the channel, if I_c is measured at a voltage V, I_t is the value expected at voltage $V + \Delta\Phi$ (see Fig. 1 *C*).

RESULTS

Effects of $[Ba^{2+}]_o$

We began by examining the current-voltage (*I-V*) relations for whole-cell currents using different concentrations of Ba^{2+} as the charge carrier. Fig. 2 shows representative currents, and tail currents after partial repolarization, in 2 mM Ba^{2+} and 50 mM Ba^{2+}. Current amplitudes are clearly increased in 50 mM Ba^{2+} (note scale bars in Fig. 2, *A* and *B*). The peak current saturated as a function of $[Ba^{2+}]_o$, with an apparent K_d of 11.6 mM (Fig. 2 *D*).

Surface charge and gating. High $[Ba^{2+}]_o$ also shifts the peak current to more positive voltages (Fig. 2 *C*). The shift in *I-V* relations can be explained by screening of negative surface charges by Ba^{2+}: charge screening makes the extracellular surface potential less negative, so the voltage across the channel is more negative, and stronger depolarization would be required to open the channel in high $[Ba^{2+}]_o$. $\Delta\Phi$, the change in surface potential, can be estimated from the shift in the activation curve, measured from tail currents such as those in Fig. 2 *B*. The shift of activation curves to more positive voltages with increasing $[Ba^{2+}]_o$ (Fig. 3 *A*) can be well described by Gouy-Chapman theory, with a surface charge density σ = 1 e^-/140 Å^2 (Fig. 3 *B*), assuming that Ba^{2+} ions act entirely by charge screening. If Ba^{2+} is

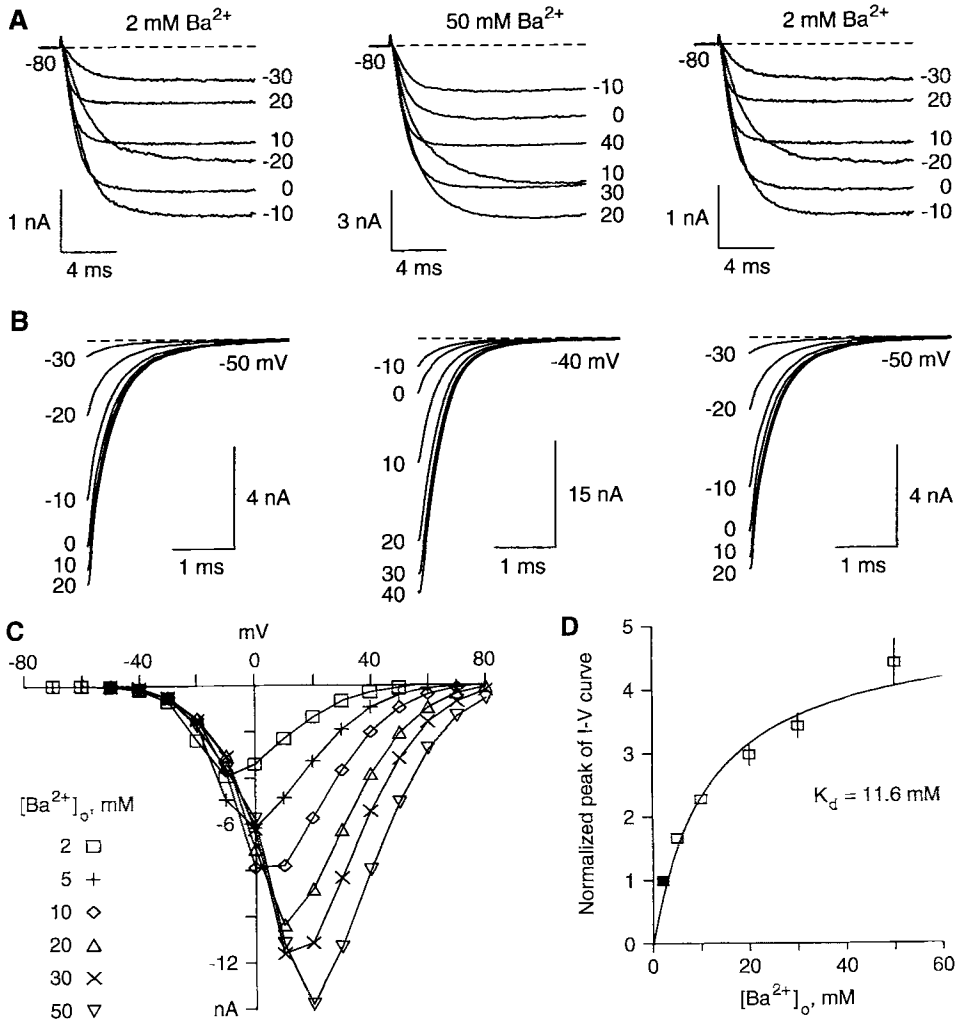

FIGURE 2. Effect of Ba^{2+} on whole-cell currents. (*A*) Currents recorded during voltage steps from a holding potential of −80 mV. The currents shown were recorded in 2 mM Ba^{2+} (*left*), 50 mM Ba^{2+} (*middle*), and after return to 2 mM Ba^{2+} (*right*). (*B*) Tail currents, from the same experiment as *A* , recorded after repolarization to −50 mV (2 mM Ba^{2+}) or −40 mV (50 mM Ba^{2+}). The voltage during the previous step is indicated at the left of each record. Note that the time and current scales are different in *A* and *B*. (*C*) Current-voltage relations in different $[Ba^{2+}]_o$, from the same cell as *A* and *B*. Currents were measured at the end of each voltage step. To correct for rundown, currents were measured alternately in control and test (higher Ba^{2+}) solutions. The control currents recorded before and after each test solution were scaled up to match the initial control current, and the currents in the test solution were scaled up using the average of those two scaling factors. In the cell shown, peak current in 2 mM Ba^{2+} decreased by 35% over the entire 50-min protocol, and the actual peak current in 50 mM Ba^{2+} was 9 nA. (*D*) The relation between the peak of the *I-V* curve and $[Ba^{2+}]_o$. Because voltage steps were given in 10-mV increments, the peak was estimated for each *I-V* curve by a cubic spline interpolation with an interval of 1 mV. The solid curve is the least-squares fit for a single binding site. Values are the average (±SEM) from four cells. Currents were normalized to the value at 2 mM Ba^{2+} in each cell (*solid box*).

assumed to also bind to the surface charges, a lower σ is obtained, with little or no improvement in the fit to the data (Fig. 3 *B*).

Surface charge and permeation. Surface potentials could affect the current-$[Ba^{2+}]_o$ relationship in two ways. First, because gating is affected, the probability that a channel is open, measured at a particular voltage, would vary with $[Ba^{2+}]_o$. Thus, the increase in current with $[Ba^{2+}]_o$ will depend on the voltage at which the current is measured. At certain negative voltages, the current actually decreases in high $[Ba^{2+}]_o$ (Fig. 2 *C*). Second, a surface potential would increase the local $[Ba^{2+}]_o$, and would shift the energy profile seen by an ion in the channel, thus affecting ion permeation. Interpretation of the current-$[Ba^{2+}]_o$ relationship as saturation of a binding site within the channel pore requires evaluation of both of these effects of surface charge. And as discussed in detail below, it is possible that the surface charge seen by the voltage sensors (Fig. 3 *B*) differs from the surface charge seen by the channel pore.

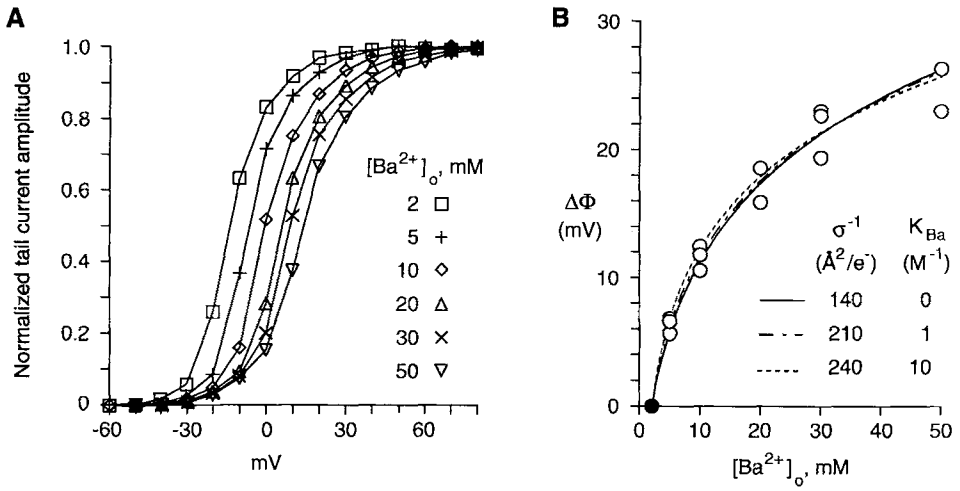

FIGURE 3. The shift in gating with $[Ba^{2+}]_o$. (*A*) Activation curves were measured from tail currents, including those in Fig. 2 *B*, as described in Methods. (*B*) The shift of the midpoint of the activation curve as a function of $[Ba^{2+}]_o$, measured relative to the control activation curve in 2 mM Ba^{2+} (*solid symbol*). The curves are fits to the data, calculated from the Grahame equation (Eqs. 1 and 2), assuming the indicated values of K_{Ba}. Data are from three cells.

To reduce uncertainty resulting from shifts in the activation curve, instantaneous *I-V* relations were measured after large depolarizations, which should produce maximal channel activation. Sample tail current records using this protocol (Fig. 4 *A*), and instantaneous *I-V* relations measured from the tail currents (Fig. 4 *B*), demonstrate a large increase in slope conductance with $[Ba^{2+}]_o$. The instantaneous currents measured at 0 mV could be fitted with a K_d = 23.5 ± 3.7 mM (Fig. 4 *C*), about twice the value found for peak current as a function of $[Ba^{2+}]_o$. The apparent K_d from instantaneous currents did not depend strongly on voltage near 0 mV (K_d = 20.2 ± 2.6 mM at −10 mV, K_d = 27.4 ± 3.1 mM at +10 mV).

A surface charge in the vicinity of the channel pore could affect the measured K_d for Ba^{2+}. To evaluate that effect, we calculated current-$[Ba^{2+}]_o$ curves "corrected"

assuming a wide range of values for σ (Fig. 5). If the channel pore and voltage sensor see the same surface charge, the instantaneous current does not saturate as a function of local $[Ba^{2+}]_o$ (Fig. 5 *C*). For higher σ, the current-$[Ba^{2+}]_o$ relation actually shows an upward curvature, and the calculated local $[Ba^{2+}]_o$ is unrealistically high (Fig. 5, *A* and *B*). For lower σ, the current-$[Ba^{2+}]_o$ relation does saturate (Fig. 5, *D–F*). The current-$[Ba^{2+}]_o$ relationship cannot be used to determine the σ seen by the channel

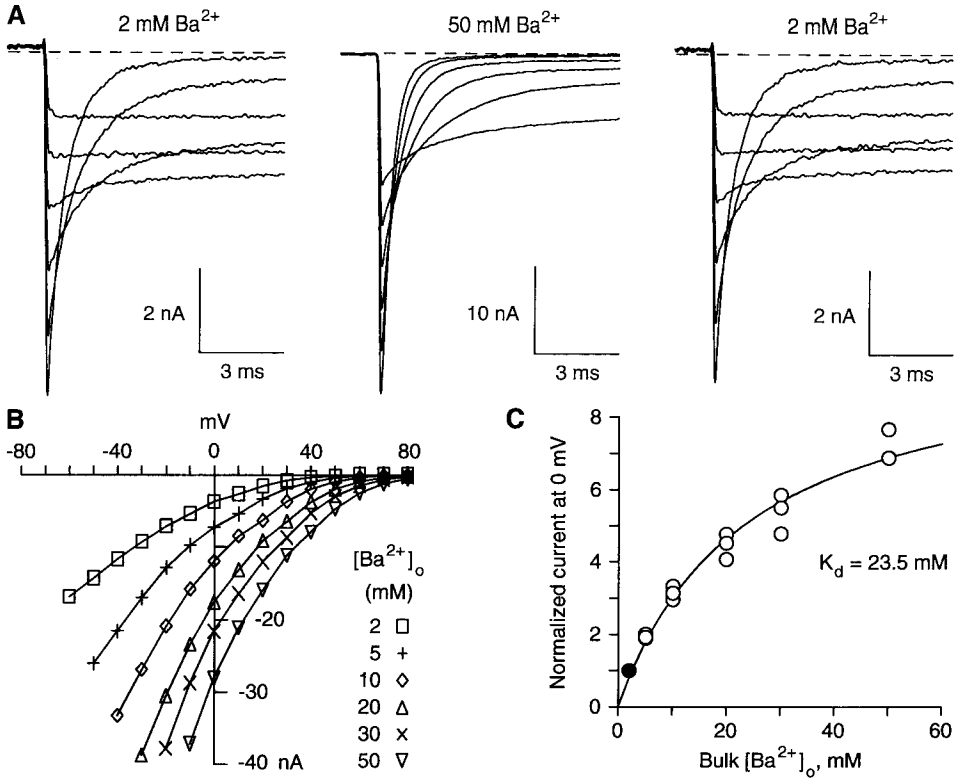

FIGURE 4. Effect of $[Ba^{2+}]_o$ on instantaneous *I-V* relations. (*A*) Tail currents recorded at voltages from −30 to +20 mV (in 10-mV increments), after depolarizing pulses to +80 mV. (*B*) Instantaneous *I-V* relations measured from tail currents, as described in Methods. The instantaneous current at 0 mV in 50 mM Ba^{2+} was −19.4 nA, before correction for rundown. (*C*) The effect of $[Ba^{2+}]_o$ on the instantaneous current at 0 mV, fitted assuming a single binding site for Ba^{2+}. Currents were normalized to the value at 2 mM Ba^{2+} (*solid symbol*), in three cells.

pore, other than to suggest an upper limit of $\sim 1\ e^-/150\ Å^2$. However, given a value for σ, the K_d can be estimated (Fig. 5 *G*).

Effects of Ionic Strength

Surface charge and gating. An independent estimate of σ can be obtained by varying the ionic strength, as monovalent ions can also screen surface charge. The effect of

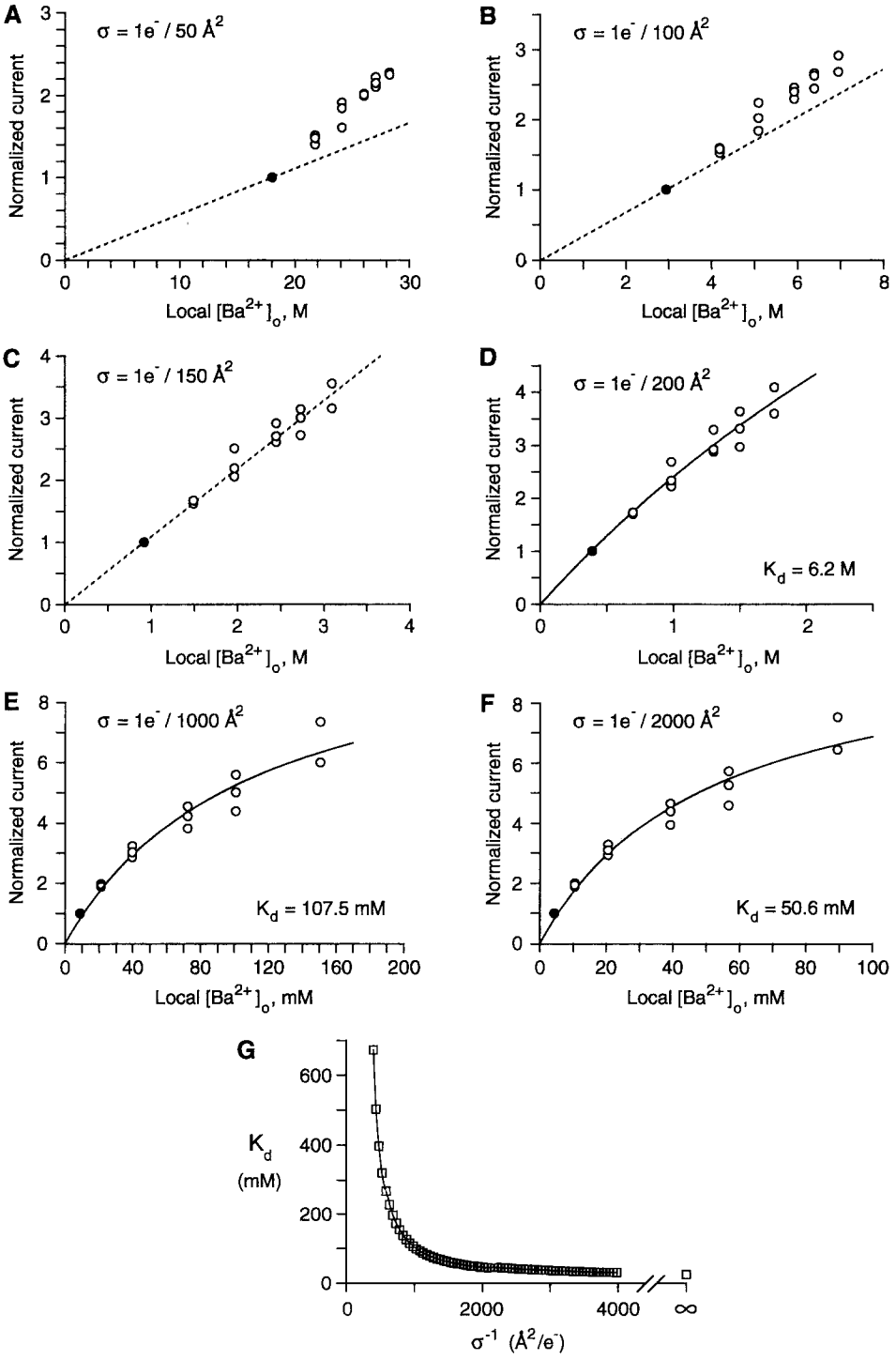
A
σ = 1e⁻ / 50 Å²
Normalized current
Local [Ba²⁺]o, M
B
σ = 1e⁻ / 100 Å²
Normalized current
Local [Ba²⁺]o, M
C
σ = 1e⁻ / 150 Å²
Normalized current
Local [Ba²⁺]o, M
D
σ = 1e⁻ / 200 Å²
Kd = 6.2 M
Normalized current
Local [Ba²⁺]o, M
E
σ = 1e⁻ / 1000 Å²
Kd = 107.5 mM
Normalized current
Local [Ba²⁺]o, mM
F
σ = 1e⁻ / 2000 Å²
Kd = 50.6 mM
Normalized current
Local [Ba²⁺]o, mM
G
Kd (mM)
σ⁻¹ (Å²/e⁻)

FIGURE 5

reducing $[NMG{\cdot}Cl]_o$ from the usual 117.5 mM to 10 mM (with sucrose added to maintain osmolarity) is shown in Fig. 6. Current amplitudes are increased in low ionic strength, and the activation curve shifts to more negative voltages (Fig. 6 *C*). The shift in the activation curve with ionic strength can be described by Gouy-Chapman theory with $\sigma = 1\ e^-/85\ Å^2$ (Fig. 6 *D*). The fit is improved slightly by assuming low affinity binding of Ba^{2+} ($K_{Ba} = 1\ M^{-1}$), but stronger binding produces a poorer fit. $\Delta\Phi$ depends on σ in a biphasic manner (Fig. 1 *B*), which might suggest that a second solution would be found at much lower σ. However, no reasonable fit could be obtained with low σ, as a value that would produce the appropriate $\Delta\Phi$ for 40 mM NMG significantly overestimated the observed $\Delta\Phi$ at 10 mM, and underestimated $\Delta\Phi$ at 250 mM. The estimate of the surface charge seen by the gating mechanism, based on changes in ionic strength ($\sigma = 1\ e^-/85\ Å^2$, Fig. 6 *D*) is within a factor of two of the estimate from changes in $[Ba^{2+}]_o$ ($\sigma = 1\ e^-/140\ Å^2$, Fig. 3 *B*).

Surface charge and permeation. We next wished to estimate the surface charge seen by the permeation mechanism. The increase in peak current at low ionic strength (Fig. 6, *A* and *B*) might reflect a change in surface potential, but the shift in the activation curve to more negative voltages (Fig. 6 *C*) would also increase the current. To distinguish those possibilities, instantaneous *I-V* relations were measured after strong depolarizations that should maximally activate channels. The instantaneous currents were also increased at low ionic strength (Fig. 7), which suggests that the channel conductance increases.

How would a surface potential affect permeation in solutions of different ionic strength? Two effects must be considered (see Methods). First, in low ionic strength, the surface potential on the extracellular side of the channel would be more negative, which would make the voltage seen by the channel more positive, decreasing the driving force on Ba^{2+}. To compare an instantaneous *I-V* to that measured in higher ionic strength, the *I-V* measured in low ionic strength should be shifted to more positive voltages (see Fig. 1 *C*). Second, although the bulk $[Ba^{2+}]_o$ was held constant in these experiments, the more negative surface potential at low ionic strength would increase the local $[Ba^{2+}]_o$, which would tend to increase the channel conductance. However, the amount of the increase would depend on whether the channel conductance saturates as a function of $[Ba^{2+}]_o$. Fortunately, although the K_d of the channel for Ba^{2+} is not known at this stage of the calculation, for a given σ, the K_d can be estimated from Fig. 5 *G*. Given a value for σ, the expected ratio of currents in solutions of different ionic strength (I_t/I_c) can be calculated from Eq. 5.

FIGURE 5. Recalculation of the instantaneous current-$[Ba^{2+}]_o$ relation, assuming various values for the surface charge seen by the channel pore. For each value of surface charge density (σ) and $[Ba^{2+}]_o$, Φ was calculated from the Grahame equation without binding (Eq. 1). Instantaneous currents were measured at voltage $\Delta\Phi$, where the voltage across the channel should be the same as at a membrane potential of 0 mV in 2 mM Ba^{2+} (see Fig. 1 *C*). Currents were normalized to the value at 2 mM Ba^{2+} in each cell. The local $[Ba^{2+}]_o$ was calculated from Eq. 3. The dashed lines (*A–C*) were drawn through the control current at bulk $[Ba^{2+}]_o = 2$ mM, and solid curves (*D–F*) were fitted to the indicated K_d values. (*G*) The fitted K_d values, as a function of the reciprocal of the assumed surface charge density ($1/\sigma$), calculated in steps of 1 $e^-/50\ Å^2$.

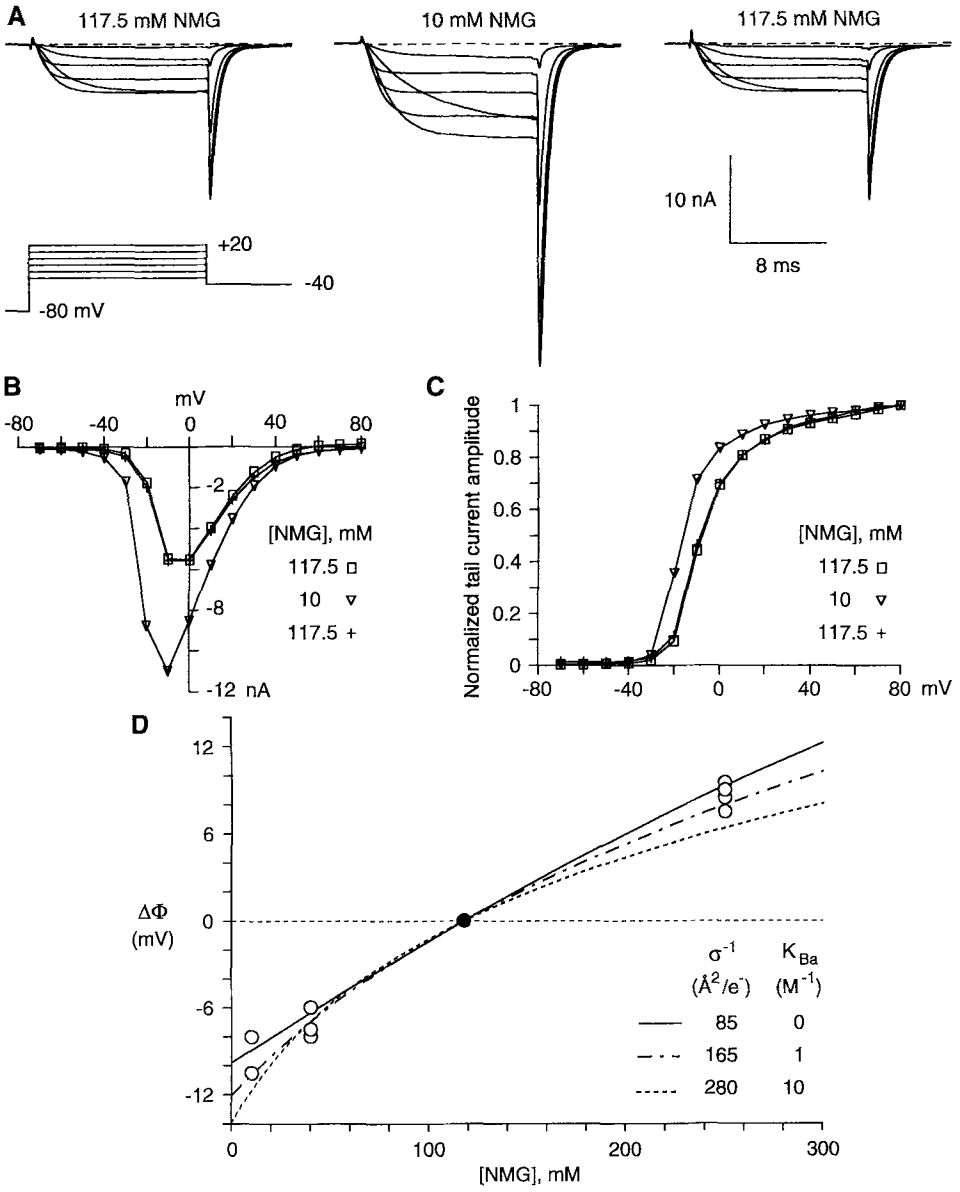

FIGURE 6. Effect of changes in $[NMG{\cdot}Cl]_o$ on whole-cell currents. (*A*) Currents in response to voltage steps from −30 to +20 mV, with tail currents at −40 mV, in control (117.5 mM NMG·Cl), in 10 mM NMG·Cl, and after return to control. See Table I for the full composition of the extracellular solutions. (*B*) The *I-V* relations and (*C*) the activation curve, for the same experiment as *A*. (*D*) Voltage shifts, measured from the midpoints of the activation curves (with respect to the control activation curve, *solid symbol*), shown as a function of $[NMG{\cdot}Cl]_o$. The lines drawn were calculated from Eqs. 1 and 2 for the parameters shown. Data are from three cells for each change in $[NMG{\cdot}Cl]_o$.

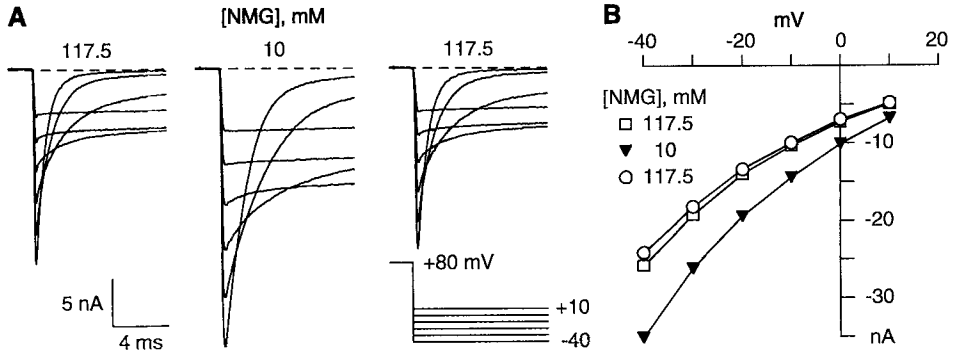

FIGURE 7. Effect of changes in $[NMG{\cdot}Cl]_o$ on instantaneous *I-V* relations. (*A*) Tail currents recorded before, during, and after a change from control to 10 mM NMG·Cl. (*B*) Instantaneous *I-V* relations, for the same experiment as *A*.

For a wide range of σ, expected I_t values were calculated from the measured I_c using Eq. 5. The goodness of fit was then evaluated by calculating the average of the squared deviations between the measured and calculated I_t values, with the results shown in Fig. 8. Because of the biphasic dependence of $\Delta\Phi$ on σ, there are two

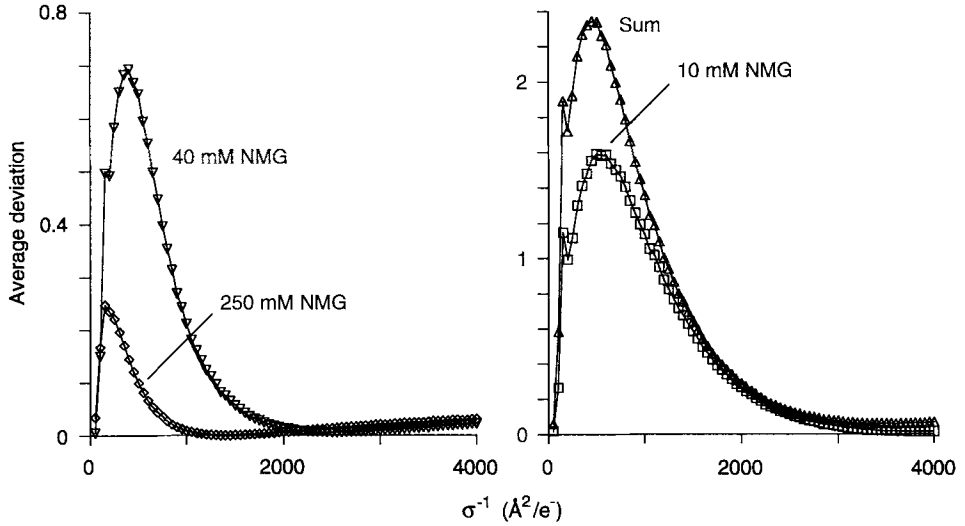

FIGURE 8. Estimation of the surface charge associated with permeation. For each set of instantaneous *I-V* curves (e.g., Fig. 7 *B*), the *I-V* in the control solution was adjusted for the effect of surface charge, for σ values from 1 $e^-/50$ Å^2 to 1 $e^-/4{,}000$ Å^2 in steps of 1 $e^-/50$ Å^2. The adjustment includes a voltage shift ($\Delta\Phi$, from Eq. 1), an increase in local $[Ba^{2+}]_o$ (Eq. 3), and correction for saturation of the pore with Ba^{2+} (from Fig. 5 *G* and Eq. 5), as described in the text. For high σ (1 $e^-/50$ Å^2 to 1 $e^-/150$ Å^2), where the current-local $[Ba^{2+}]_o$ relation does not saturate (Fig. 5 *G*), the current was assumed to be proportional to the local $[Ba^{2+}]_o$. For each σ, squared deviations were calculated between the adjusted currents and the currents measured in the test solution. Because the best fitting σ values were different for each test $[NMG{\cdot}Cl]_o$, the dependence of the average squared deviation is shown separately for each concentration, together with the sum for all three test $[NMG{\cdot}Cl]_o$ (Δ).

minima, one near 1 $e^-/50$ Å^2, and one at much lower σ. The minimum near 1 $e^-/50$ Å^2 does not seem realistic, as such high charge densities produce upwardly curving current-$[Ba^{2+}]_o$ relations (Fig. 5, *A* and *B*). The other error minimum is near 1 $e^-/1{,}500$ Å^2 for 250 mM NMG, 1 $e^-/2{,}500$ Å^2 for 40 mM, and 1 $e^-/3{,}900$ Å^2 for 10 mM. Overall, the lowest error was for 1 $e^-/3{,}400$ Å^2, but that reflects primarily the large errors for fitting the data at 10 mM (Fig. 8). All of these estimates of σ for permeation are far lower than the σ for gating. It is noteworthy that the error is near maximum at 1 $e^-/150$ Å^2, for all ionic strengths. This result suggests that the pore and the voltage sensor do not see the same surface charge.

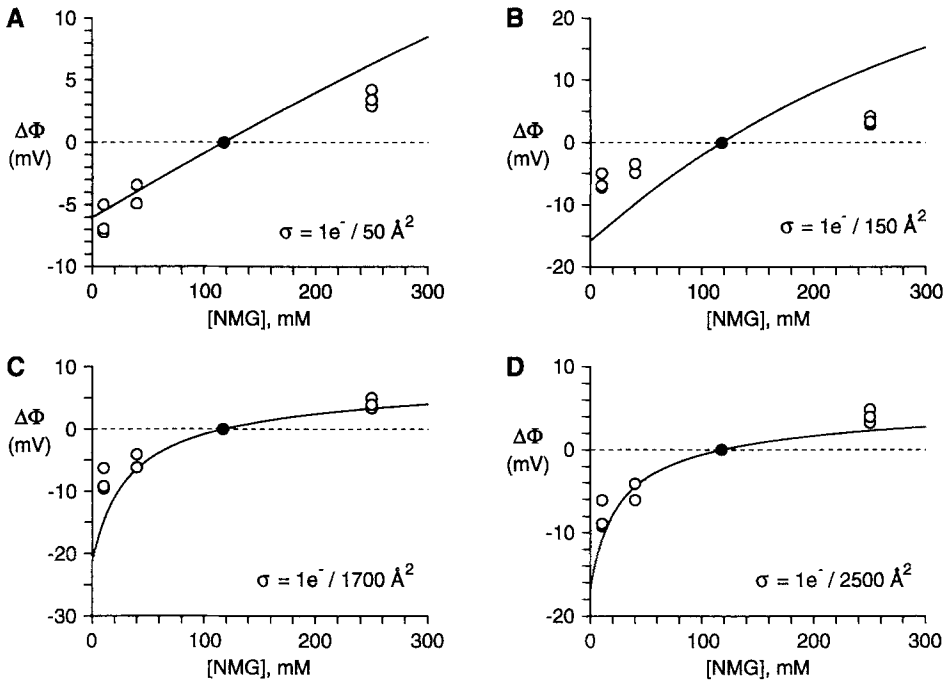

FIGURE 9. Comparison of experimental $\Delta\Phi$ values to the $\Delta\Phi$ calculated from the Grahame equation, for different assumed values of the σ for permeation. Symbols indicate the experimental $\Delta\Phi$ values, calculated as described in the text, and the solid curves were calculated from the Grahame equation. All $\Delta\Phi$ values are calculated relative to 117.5 mM NMG·Cl (*solid symbol*).

For better visual evaluation of the quality of fit, the voltage shifts associated with permeation at different ionic strength were analyzed in a different manner (Fig. 9). Here, for each value of σ, I_t values were calculated from I_c from Eq. 5, and an "experimental $\Delta\Phi$" value was calculated by shifting the calculated I_t-V curve along the voltage axis to best match the measured I_t-V curve. Fig. 9 compares these "experimental $\Delta\Phi$" values to the $\Delta\Phi$'s calculated from the Grahame equation (Eq. 1). No assumed σ could accurately describe the voltage shifts at all ionic strengths, although values of σ near 1 $e^-/2{,}000$ Å^2 gave the best fit overall. A surface charge of 1 $e^-/150$ Å^2 produced an especially poor fit at all ionic strengths. The quality of the

fits does not allow a precise estimate of the surface charge for permeation, but both methods of analysis suggest that charge densities higher than 1 e^-/1,500 $Å^2$ can be excluded. Allowing binding of Ba^{2+} to the surface charge, with K_{Ba} ranging from 0 to 80 M^{-1}, did not qualitatively affect the results.

Thus far, we have assumed that the change in instantaneous *I-V* relations with ionic strength is entirely due to a change in surface potential. However, we cannot rule out a completely different interpretation, block of calcium channel currents by NMG, the monovalent cation used in our study (see Kuo and Hess, 1992). That is, the increase in current at low ionic strength might actually reflect relief of NMG block, not effects of ionic strength per se. The change in instantaneous current can be described reasonably well by block by NMG, with a K_d of 320 mM (Fig. 10), assuming that the channel pore sees no surface charge at all. Thus, the values estimated from Figs. 8 and 9 must be considered upper limits for the amount of surface charge seen by the channel pore.

In principle, we could test the hypothesis that NMG blocks the channel by replacing NMG with a small inorganic cation (e.g., Cs^+, see Kuo and Hess, 1992), but

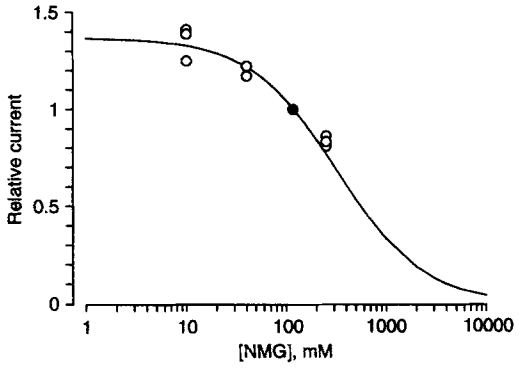

FIGURE 10. Interpretation of the effect of NMG·Cl on permeation as block by NMG. Instantaneous currents at 0 mV were normalized to the values in control (117.5 mM NMG·Cl, *solid symbol*), and were fitted assuming inhibition of the current by binding of NMG to a single site with K_d = 320 mM. No surface charge effects were considered.

there is a relatively nonselective voltage-dependent cation current in sympathetic neurons that complicates isolation of current through calcium channels in such conditions (Jones, 1987; Zhu and Ikeda, 1993). That contaminating current, and problems with recording stability, have also prevented us from studying in any detail current carried by monovalent cations through the calcium channel (Jones and Marks, 1989).

DISCUSSION

This study draws two main conclusions. (*a*) If any surface charge is associated with calcium channel permeation, it is at least 10-fold lower than that associated with gating. (*b*) After correction for the possible surface charge, the calcium channel still shows saturation with $[Ba^{2+}]_o$.

Some features of the experimental design used here are worth noting. First, the use of tail currents to measure activation curves and instantaneous *I-V* relations allowed direct separation of gating and permeation. In principle, the instantaneous

I-V contains the same information about the voltage dependence of permeation as would single-channel *I-V* relations. The one assumption is that the limiting p (open) at extreme positive voltages is unaffected by changes in $[Ba^{2+}]_o$ or ionic strength—that is, that these changes have no effect on gating other than via changes in surface potential. Comparable experiments on single N channels would be difficult, as their gating is rapid, and channel activity runs down rapidly in excised patches, which would normally be used for experiments where the extracellular solution must be changed. In addition, the single-channel basis of the whole-cell N current is now open to question (Elmslie et al., 1994).

We have used two independent methods to screen surface charge, changes in permeant ion concentration, and changes in ionic strength. These have very different consequences for changes in surface potential (Fig. 1, *A* and *B*). When only the permeant ion concentration is varied, the results can often be interpreted either as effects of surface charge or as effects on permeation per se. In principle, and to some extent in practice, data on ionic strength can resolve that ambiguity.

Surface Charge and Gating

From the shift in activation kinetics with $[Ba^{2+}]_o$, we estimated a surface charge of 1 $e^-/140$ Å^2 from Gouy-Chapman theory, assuming no binding of Ba^{2+} to the surface charge. This is in the range of previous reports for several different calcium channels (1 $e^-/80$ Å^2, Ohmori and Yoshi, 1977; 1 $e^-/80$ Å^2, Wilson et al., 1983; 1 $e^-/500$ Å^2, Cota and Stefani, 1984; 1 $e^-/200$ Å^2, Byerly et al., 1985; 1 $e^-/250$ Å^2, Kass and Krafte, 1987), including estimates assuming a nonzero K_{Ba} (1 $e^-/435$ Å^2 with K_{Ba} = 18 M^{-1}, Kostyuk, Mironov, Doroshenko, and Ponomarev, 1982; 1 $e^-/200$ Å^2 with K_{Ba} = 5.5 M^{-1}, Ganitkevich et al., 1988; 1 $e^-/185$ Å^2 with K_{Ba} = 2.3 M^{-1}, Smith et al., 1993). As noted previously (Kostyuk et al., 1982; Ganitkevich et al., 1988), the experimentally measured voltage shifts can be fitted either with a small (or zero) association constant, or with a higher association constant and a lower charge density. For our data, relatively high affinity binding (K_{Ba} = 10 M^{-1}) would decrease the estimated surface charge density from 1 $e^-/140$ Å^2 to 1 $e^-/240$ Å^2 (Fig. 3 *B*).

Experiments varying ionic strength provided an independent measure of the surface charge density associated with gating, 1 $e^-/85$ Å^2. That agrees reasonably well with the estimate from changes in $[Ba^{2+}]_o$. However, Becchetti et al. (1992) reported 1 $e^-/1{,}000$ Å^2 in rat sensory neurons, based on changes in ionic strength. The reason for this discrepancy is not clear. Their voltage shift estimates were reduced considerably by corrections for junction potentials (Table I of Becchetti et al., 1992). In our ionic strength experiments, correction for junction potentials was not necessary, as there is no electrode-bath junction potential in the whole-cell configuration, and we used a 3-M KCl agar bridge as reference. There is also a potential ambiguity between low and high charge density solutions to the Grahame equation, for experiments varying ionic strength (Fig. 1 *B*), but our data could not be adequately fitted by a low charge density (see Results).

The voltage shifts with ionic strength could be fitted well with values of K_{Ba} from 0 to 1 M^{-1}, but not with higher affinity binding (Fig. 6 *D*). This suggests that Ba^{2+} binds weakly if at all to the surface charge associated with gating. Thus, most or all of the effect of Ba^{2+} on surface charge is by screening. Consistent with this, we find that

the shift in the activation curve with Mg^{2+} is similar to that produced by Ba^{2+} (6.0 ± 0.1 mV between 2 mM Ba^{2+} and 2 mM Ba^{2+} + 3 mM Mg^{2+}, mean ± SEM, n = 3; 6.4 ± 0.4 mV between 2 and 5 mM Ba^{2+}, see Fig. 3 *B*), so there is no need to postulate specific effects of these ions on surface charge.

Surface Charge and Permeation

Our data cannot provide a firm estimate for the surface charge associated with permeation, but some possibilities can be excluded. First, the effects of ionic strength cannot be well described by intermediate surface charge densities (~ 1 e^-/100 Å^2 to 1 e^-/1,500 Å^2, Figs. 8 and 9). Higher surface charge densities are unlikely, as they predict upwardly curving current-$[Ba^{2+}]_o$ relations, with local $[Ba^{2+}]_o$ of 3–30 M (Fig. 5). The effects of changes in NMG can be interpreted either as block by NMG, with no surface charge effect (Fig. 10), or as the effect of a relatively small amount of surface charge (~ 1 e^-/2,000 Å^2, Figs. 8 and 9). Of course, it is possible that the effects of NMG involve a combination of block and charge screening, in which case the estimated surface charge would be less than 1 e^-/2,000 Å^2 (not shown). Overall, our data are most consistent with surface charge densities <1 e^-/1,500 Å^2, and cannot rule out the total absence of surface charge associated with permeation. This allows the conclusion that there is less surface charge associated with permeation than with gating, by at least a factor of 10.

Preliminary experiments on the effects of pH also support this conclusion. There was no effect on the instantaneous *I-V* from pH 7.2 to 9.0, even though the activation curve is shifted in that pH region as expected from titration of the surface charge associated with gating (data not shown).

Several previous studies have also concluded that screening of surface charge has a larger effect on gating of voltage-dependent channels than on permeation (Begenisich, 1975; Wilson et al., 1983; Coronado and Affolter, 1986; Yue and Marban, 1990; Kuo and Hess, 1992; Ji, Weiss, and Langer, 1993). Most estimates of the surface charge density seen by the channel pore are low (1 e^-/1,400 Å^2, MacKinnon et al., 1989; 1 e^-/650 Å^2, Kuo and Hess, 1992; 1 e^-/2,500 Å^2, Naranjo and Latorre, 1993). One exception is Smith et al. (1993) who reported a surface charge density of 1 e^-/167 Å^2 (K_{Ba} = 0 M^{-1}) or 1 e^-/71 Å^2 (K_{Ba} = 77 M^{-1}) for L-type calcium channels. That estimate was based on fitting single-channel *I-V* curves in different $[Ba^{2+}]_o$ to the Goldman-Hodgkin-Katz current equation, allowing for a voltage shift, which was interpreted as an effect of surface charge. It seems likely that the shape of the single-channel *I-V* curves could be explained in other ways. We also note that our upper limit of 1 e^-/1,500 Å^2 is even lower than the value from Kuo and Hess (1992) for L channels.

Nature of the Surface Charge

We find that more surface charge is associated with gating than with permeation. One simple interpretation is that the mouth of the channel is located at some distance from the surface charge (Apell, Bamberg, and Laüger, 1979; Bell and Miller, 1984; Coronado and Affolter, 1986), as expected for a protein molecule with a relatively large extracellular domain, probably including an outer vestibule (see review by Latorre and Miller, 1983). In contrast, the voltage sensors controlling channel gating

must be located within the membrane field, presumably in a region of low dielectric, where the effects of remote charged groups would be relatively strong.

Our data do not address the physical nature of the surface charge. Studies varying the lipid composition in planar bilayers (Bell and Miller, 1984; Moczydlowski, Alvarez, Vergara, and Latorre, 1985; Coronado and Affolter, 1986; Cukierman, Zinkand, French, and Krueger, 1988), or using chemical reagents to modify surface charges (MacKinnon and Miller, 1989; MacKinnon et al., 1989; Ji et al., 1993), have found evidence for both charges on the membrane lipid and charges on the channel protein itself. One intriguing possibility is that negatively charged groups in the outer vestibule of the channel constitute a surface charge, which could enhance permeation by increasing the local cation concentration near the pore. Because divalent cations are selectively attracted, in principle this effect could contribute to the selectivity of calcium channels for divalent cations. However, as concluded by Kuo and Hess (1992), the low effective surface charge associated with permeation in calcium channels implies that electrostatic attraction of cations is a relatively minor effect.

The observation that gating and permeation see different amounts of surface charge means that the assumptions of Gouy-Chapman theory are not satisfied here. That is not really surprising, as the assumption of a uniform planar surface charge is not realistic for an ion channel. The nonlinear Poisson-Boltzmann equation could provide a more accurate description of the surface potential produced by discretely distributed charges (Dani, 1986; reviewed by Green and Anderson, 1991). We did not develop that approach here, in part because the distribution of charge on (and near) the calcium channel is not known. Qualitatively, a model that places the surface charge at a distance from the channel pore predicts that Gouy-Chapman theory would be a good approximation at high ionic strength, but would overestimate the change in surface potential in low ionic strength solutions (Cai and Jordan, 1990). This might explain the poor fit of Gouy-Chapman theory to our data on permeation at low ionic strength (Fig. 9, *C* and *D*).

The voltage shifts associated with gating could be described well by Gouy-Chapman theory, as others have found previously. However, it is possible that the difference between surface charge estimates from changes in $[Ba^{2+}]_o$ vs changes in ionic strength (1 e^-/140 Å^2 vs 1 e^-/85 Å^2) reflects limitations of Gouy-Chapman theory.

Saturation of the Calcium Channel with Ba^{2+}

The peak inward current as a function of $[Ba^{2+}]_o$ could be described by an apparent K_d of 11.6 mM (Fig. 2 *D*). That is in good agreement with values for other calcium channels (8–12.5 mM, Cota and Stefani, 1984; 9.6 mM, Ganitkevich et al., 1988). In contrast, the apparent K_d from instantaneous *I-V* relations was 23.5 mM. K_d values from single-channel measurements are variable, but generally comparable (40 mM, Coronado and Affolter, 1986; 28 mM, Hess, Lansman, and Tsien, 1986; 13 mM, Rosenberg, Hess, and Tsien, 1988; 5.5 mM, Smith et al., 1993). Kuo and Hess (1993) found a K_d of 6 mM for the conductance-Ba^{2+} activity relationship, which would correspond roughly to a concentration of 16 mM (see Hess and Tsien, 1984). Our data could be fitted adequately by a single binding site, at least over the 25-fold concentration range examined (Fig. 4 *C*), which was not true in some previous studies (Yue and Marban, 1990; Smith et al., 1993). Deviations from a simple hyperbolic

relation could result from multiple ion occupancy and ion–ion interactions within the pore, or from effects of surface charge, and could explain some of the variability among K_d estimates. On the other hand, multiple binding sites need not produce complex current-concentration relationships. For example, the Almers and McCleskey (1984) two-site three-barrier model for calcium channel permeation produces an almost perfect hyperbolic relationship between current and Ba^{2+} (at 0 mV), while the very similar Hess and Tsien (1984) model is better described by the sum of two components, with the higher affinity component ~7% of the total current (calculations not shown).

It is interesting that the apparent K_d measured from the peak current is lower than that measured from the instantaneous *I-V* relationship. If the channel open probability were the same at the peak of each *I-V* curve, the two K_d measurements might

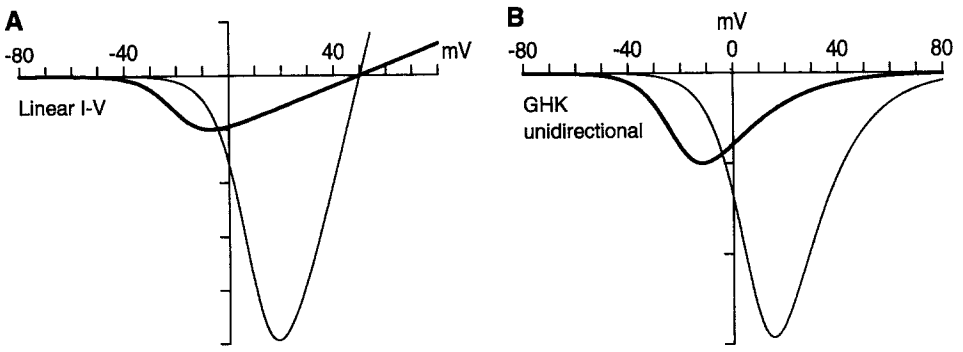

FIGURE 11. Simulation of the effect on I-V relations of a surface charge associated solely with gating. The channel open probability was assumed to follow a Boltzmann relation, with four charges per channel (e-fold for 25/4 mV). Half-maximal activation was at −20 mV (*thick curves*) or +10 mV (*thin curves*). Current flow through an open channel was assumed to depend linearly on voltage with a reversal potential of +50 mV (*A*), or to follow the Goldman-Hodgkin-Katz current equation, considering Ba^{2+} influx without efflux (*B*). At each voltage, the single-channel current was assumed to be 10-fold higher for the thinner curves. Absolute current levels are arbitrary.

agree. It has been argued that screening of surface charge should move the *I-V* curve along the voltage axis without change in shape, if the permeation and gating mechanisms are affected equally (see Wilson et al., 1983; Byerly et al., 1985). Because the macroscopic current is the product of the activation curve times the instantaneous *I-V* curve (i.e., the channel open probability × the current when all channels are open), if both are shifted by $\Delta\Phi$ mV, the steady state *I-V* curve would also shift by $\Delta\Phi$ mV. Thus, the channel open probability, measured at the voltage producing peak inward current, would be the same regardless of $[Ba^{2+}]_o$.

But what if gating is shifted more than permeation? Fig. 11 shows the effect of a simulated increase in $[Ba^{2+}]_o$, where the instantaneous *I-V* curve is increased 10-fold, the activation curve is shifted to more positive voltages by 30 mV, and the channel pore is assumed to see no surface charge. Assuming that the open channel has a

linear *I-V*, with a reversal potential of +50 mV, the peak inward current increases not 10-fold but fivefold (Fig. 11 *A*). Qualitatively, this result seems independent of the mechanism of permeation, as the peak inward current increases only threefold if the open channel shows Goldman-Hodgkin-Katz rectification (Fig. 11 *B*). Thus, a graph of peak inward current vs $[Ba^{2+}]_o$ would underestimate the increase in open-channel conductance with $[Ba^{2+}]_o$, which would make the relation appear to saturate more strongly.

On the other hand, the shift in peak current and the shift in the midpoint of the activation curve are quite similar, even if the pore does not see any surface charge. For the assumed 30-mV shift of activation kinetics in Fig. 11, the peak current shifted by 26 mV (linear *I-V*) or 27 mV (GHK rectification). Thus, it should be a good approximation to use shifts in the point of peak inward current to estimate the effect of surface charge on activation kinetics, as in several previous studies.

Some previous studies concluded that the apparent saturation of the calcium channel with Ba^{2+} could be attributed largely (Cota and Stefani, 1984; Smith et al., 1993) or entirely (Ohmori and Yoshii, 1977; Wilson et al., 1983; Byerly et al., 1985; Ganitkevich et al., 1988) to the effect of surface charge, without need for a saturable Ba^{2+} binding site within the channel pore, if permeation and gating see comparable amounts of surface charge. For our upper limit of 1 e^-/1,500 Å^2 for permeation, the K_d changes from 23.5 mM to 65 mM, as a function of local $[Ba^{2+}]_o$. For lower surface charge densities, the K_d would approach the uncorrected value of 23.5 mM. We conclude that the K_d would be underestimated if surface charge is not considered (especially if the peak *I-V* relation is used), but the observed saturation cannot be entirely attributed to surface charge effects. The most natural interpretation of the saturation remaining after correction for surface charge is binding of Ba^{2+} to site(s) within the channel pore.

We thank Dr. Carlos A. Obejero-Paz for helpful discussions on surface potentials.

Supported in part by NIH grant NS 24471 to S. W. Jones, who is an Established Investigator of the American Heart Association.

Original version received 13 June 1994 and accepted version received 23 December 1994.

REFERENCES

Almers, W., and E. W. McCleskey. 1984. Non-selective conductance in calcium channels of frog muscle: calcium selectivity in a single-file pore. *Journal of Physiology.* 353:585–608.

Apell, H.-J., E. Bamberg, and P. Laüger. 1979. Effects of surface charge on the conductance of the gramicidin channel. *Biochimica et Biophysica Acta.* 552:369–378.

Becchetti, A., A. Arcangeli, M. R. Del Bene, M. Olivotto, and E. Wanke. 1992. Intra and extracellular surface charges near Ca^{2+} channels in neurons and neuroblastoma cells. *Biophysical Journal.* 63:954–965.

Begenisich, T. 1975. Magnitude and location of surface charges on *Myxicola* giant axons. *Journal of General Physiology.* 66:47–65.

Bell, J. E., and C. Miller. 1984. Effects of phospholipid surface charge on ion conduction in the K^+ channel of sarcoplasmic reticulum. *Biophysical Journal.* 45:279–287.

Boland, L. M., J. A. Morill, and B. P. Bean. 1994. ω-Conotoxin block of N-type calcium channels in frog and rat sympathetic neurons. *Journal of Neuroscience.* 14:5011–5027.

Byerly, L., P. B. Chase, and J. R. Stimers. 1985. Permeation and interaction of divalent cations in calcium channels of snail neurons. *Journal of General Physiology.* 85:491–518.

Cai, M., and P. C. Jordan. 1990. How does vestibule surface charge affect ion conduction and toxin binding in a sodium channel? *Biophysical Journal.* 57:883–891.

Coronado, R., and H. Affolter. 1986. Insulation of the conduction pathway of muscle transverse tubule calcium channels from the surface charge of bilayer phospholipid. *Journal of General Physiology.* 87:933–953.

Cota, G., and E. Stefani. 1984. Saturation of calcium channels and surface charge effects in skeletal muscle fibres of the frog. *Journal of Physiology.* 351:135–154.

Cukierman, S., W. C. Zinkand, R. J. French, and B. K. Krueger. 1988. Effects of membrane surface charge and calcium on the gating of rat brain sodium channels in planar bilayers. *Journal of General Physiology.* 92:431–447.

Dani, J. A. 1986. Ion-channel entrances influence permeation. Net charge, size, shape, and binding considerations. *Biophysical Journal.* 49:607–618.

Elmslie, K. S., P. J. Kammermeier, and S. W. Jones. 1994. Reevaluation of Ca^{2+} channel types and their modulation in bullfrog sympathetic neurons. *Neuron.* 13:217–228.

Frankenhaeuser, B., and A. L. Hodgkin. 1957. The action of calcium on the electrical properties of squid axons. *Journal of Physiology.* 137:218–244.

Ganitkevich, V. Ya., M. F. Shuba, and S. V. Smirnov. 1988. Saturation of calcium channels in single isolated smooth muscle cells of guinea-pig taenia caeci. *Journal of Physiology.* 399:419–436.

Gilbert, D. L., and G. Ehrenstein. 1969. Effect of divalent cations on potassium conductance of squid axons: determination of surface charge. *Biophysical Journal.* 9:447–463.

Grahame, D. C. 1947. The electrical double layer and the theory of electrocapillarity. *Chemical Reviews.* 41:441–501.

Green, W. N., and O. S. Andersen. 1991. Surface charges and ion channel function. *Annual Review of Physiology.* 41:341–359.

Green, W. N., L. B. Weiss, and O. S. Andersen. 1987. Batrachotoxin-modified sodium channels in planar lipid bilayers. Ion permeation and block. *Journal of General Physiology.* 89:841–872.

Hamill, O. P., A. Marty, E. Neher, B. Sakmann, and F. J. Sigworth. 1981. Improved patch-clamp techniques for high-resolution current recording from cells and cell-free membrane patches. *Pflügers Archiv.* 391:85–100.

Hess, P., J. B. Lansman, and R. W. Tsien. 1986. Calcium channel selectivity for divalent and monovalent cations. Voltage and concentration dependence of single-channel current in ventricular heart cells. *Journal of General Physiology.* 88:293–319.

Hess, P., and R. W. Tsien. 1984. Mechanism of ion permeation through calcium channels. *Nature.* 309:453–456.

Hille, B. 1968. Charges and potentials at the nerve surface. Divalent ions and pH. *Journal of General Physiology.* 51:221–236.

Hille, B. 1992. Ionic Channels of Excitable Membranes. Sinauer Associates Inc., Sunderland, MA. 607 pp.

Hille, B., A. M. Woodhull, and B. I. Shapiro. 1975. Negative surface charge near sodium channels of nerve: divalent ions, monovalent ions, and pH. *Philosophical Transactions of the Royal Society of London.* B270:301–318.

Ji, S., J. N. Weiss, and G. A. Langer. 1993. Modulation of voltage-dependent sodium and potassium currents by charged amphiphiles in cardiac ventricular myocytes. Effects via modification of surface potential. *Journal of General Physiology.* 101:355–375.

Jones, S. W. 1987. Sodium currents in dissociated bull-frog sympathetic neurones. *Journal of Physiology.* 389:605–627.

Jones, S. W., and K. S. Elmslie. 1992. Separation and modulation of calcium currents in bullfrog sympathetic neurons. *Canadian Journal of Physiology and Pharmacology.* 70:S56–S63.

Jones, S. W., and T. N. Marks. 1989. Calcium currents in bullfrog sympathetic neurons. I. Activation kinetics and pharmacology. *Journal of General Physiology.* 94:151–167.

Kass, R. S., and D. S. Krafte. 1987. Negative surface charge density near heart calcium channels. Relevance to block by dihydropyridines. *Journal of General Physiology.* 89:629–644.

Kostyuk, P. G., S. L. Mironov, P. A. Doroshenko, and V. N. Ponomarev. 1982. Surface charges on the outer side of mollusc neuron membrane. *Journal of Membrane Biology.* 70:171–179.

Kuffler, S. W., and T. J. Sejnowski. 1983. Peptidergic and muscarinic excitation at amphibian sympathetic synapses. *Journal of Physiology.* 341:257–278.

Kuo, C.-C., and P. Hess. 1992. A functional view of the entrances of L-type Ca^{2+} channels: estimates of the size and surface potential at the pore mouths. *Neuron.* 9:515–526.

Kuo, C.-C., and P. Hess. 1993. Characterization of the high-affinity Ca^{2+} binding sites in the L-type Ca^{2+} channel pore in rat phaeochromocytoma cells. *Journal of Physiology.* 466:657–682.

Latorre, R., and C. Miller. 1983. Conduction and selectivity in potassium channels. *Journal of Membrane Biology.* 71:11–30.

MacKinnon, R., R. Latorre, and C. Miller. 1989. Role of surface electrostatics in the operation of a high-conductance Ca^{2+}-activated K^+ channel. *Biochemistry.* 28:8092–8099.

MacKinnon, R., and C. Miller. 1989. Functional modification of a Ca^{2+}-activated K^+ channel by trimethyloxonium. *Biochemistry.* 28:8087–8092.

McLaughlin, S. 1977. Electrostatic potentials at membrane-solution interfaces. *Current Topics in Membranes and Transport.* 9:71–144.

Moczydlowski, E., O. Alvarez, C. Vergara, and R. Latorre. 1985. Effect of phospholipid surface charge on the conductance and gating of a Ca^{2+}-activated K^+ channel in planar lipid bilayers. *Journal of Membrane Biology.* 83:273–282.

Naranjo, D., and R. Latorre. 1993. Ion conduction in substates of the batrachotoxin-modified Na^+ channel from toad skeletal muscle. *Biophysical Journal.* 64:1038–1050.

Naranjo, D., R. Latorre, D. Cherbavaz, P. McGill, and M. F. Schumaker. 1994. A simple model for surface charge on ion channel proteins. *Biophysical Journal.* 66:59–70.

Ohmori, H., and M. Yoshii. 1977. Surface potential reflected in both gating and permeation mechanisms of sodium and calcium channels of the tunicate egg cell membrane. *Journal of Physiology.* 267:429–463.

Ravindran, A., H. Kwiecinski, O. Alvarez, G. Eisenman, and E. Moczydlowski. 1992. Modeling ion permeation through batrachotoxin-modified Na^+ channels from rat skeletal muscle with a multi-ion pore. *Biophysical Journal.* 61:494–508.

Rosenberg, R. L., P. Hess, and R. W. Tsien. 1988. Cardiac calcium channels in planar lipid bilayers. L-type channels and calcium-permeable channels open at negative membrane potentials. *Journal of General Physiology.* 92:27–54.

Smith, P. A., F. M. Ashcroft, and C. M. S. Fewtrell. 1993. Permeation and gating properties of the L-type calcium channel in mouse pancreatic β cells. *Journal of General Physiology.* 101:767–797.

Werz, M. A., K. S. Elmslie, and S. W. Jones. 1993. Phosphorylation enhances inactivation of N-type calcium channel current in bullfrog sympathetic neurons. *Pflügers Archiv.* 424:538–545.

Wilson, D. L., K. Morimoto, Y. Tsuda, and A. M. Brown. 1983. Interaction between calcium ions and surface charge as it relates to calcium currents. *Journal of Membrane Biology.* 72:117–130.

Yue, D. T., and E. Marban. 1990. Permeation in the dihydropyridine-sensitive calcium channel. Multi-ion occupancy but no anomalous mole-fraction effect between Ba^{2+} and Ca^{2+}. *Journal of General Physiology.* 95:911–939.

Zhu, Y., and S. R. Ikeda. 1993. Anomalous permeation of Na^+ through a putative K^+ channel in rat superior cervical ganglion neurons. *Journal of Physiology.* 468:441–461.